

Mechanism of reduction of fretting fatigue limit caused by hydrogen gas in SUS304 austenitic stainless steel

Kubota, Masanobu

Department of Mechanical Engineering, Kyushu University and National Institute of Advanced Industrial Science and Technology

Kuwada, Kyohei

Graduate School of Kyushu University

Tanaka, Yasuhiro

Mitsubishi Heavy Industries Ltd.

Kondo, Yoshiyuki

Department of Mechanical Engineering, Kyushu University and National Institute of Advanced Industrial Science and Technology

<https://hdl.handle.net/2324/25603>

出版情報 : Tribology International. 44 (11), pp.1495-1502, 2011-10. Elsevier

バージョン :

権利関係 : (C) 2010 Elsevier Ltd.



Mechanism of reduction of fretting fatigue limit caused by hydrogen gas in SUS304 austenitic stainless steel

Masanobu Kubota^{a*}, Kyohei Kuwada^b, Yasuhiro Tanaka^c, Yoshiyuki Kondo^a

^a *Department of Mechanical Engineering, Kyushu University
and National Institute of Advanced Industrial Science and Technology,
744 Motoooka, Nishi-ku, Fukuoka, 819-0395 Japan*

^b *Graduate School of Kyushu University, 744 Motoooka, Nishi-ku, Fukuoka, 819-0395 Japan*

^c *Mitsubishi Heavy Industries Ltd., Sagamihara, Tama, 229-1193 Japan*

*Corresponding author. Tel.: +81 92 802 3284; fax: +81 92 802 0001.

E-mail address: kubota@mech.kyushu-u.ac.jp (M. Kubota).

Abstract: The fretting fatigue strength of pre-strained SUS304 is reduced in hydrogen gas. The mechanism of the reduction was discussed. In hydrogen gas, local adhesion between contacting surfaces occurred and many small cracks were formed at the adhered spots. The major crack propagated from one of the small cracks. The roles of the adhesion in relation to the initiation and propagation of the small cracks were examined by a two-step environment test. When adhesion was prevented by an oxidized film, no failure of the specimen occurred. It can be presumed that the stress conditions were severer in hydrogen gas than that in air due to local adhesion.

Keywords: Fretting fatigue, Hydrogen, Adhesion, Small crack, Austenitic stainless steel

1. Introduction

Hydrogen has been recognized as a clean, efficient and renewable energy source. The utilization of hydrogen is one of the keys to achieve the sustainability of human life. It is important to clarify the effect of hydrogen on the strength of the materials to safely use hydrogen. The use of hydrogen has been very limited until today. However, hydrogen will be prevalent in our daily life with fuel cell cars and residential fuel cells. Therefore, further research is necessary to ensure the safety of hydrogen utilization machines, although there has been many studies on the detrimental effects of hydrogen on the strength of materials such as hydrogen embrittlement, delayed failure, stress-corrosion cracking, weld hydrogen cracking, etc.

The authors reported the effect of hydrogen on fretting fatigue strength. The materials were an aluminum alloy [1], low alloy steel [2], precipitation hardened stainless steel [2], and austenitic stainless steels [1][3][4]. Some of these materials showed a significant reduction of fretting fatigue strength due to hydrogen. Figure 1 is an example that shows the effect of hydrogen on the fretting fatigue strength [4]. The material was pre-strained SUS304 austenitic stainless steel and the fretting fatigue test was performed with push-pull loading. The fretting fatigue strength of the hydrogen uncharged specimen tested in air, which is represented by the solid symbols in the graph, was the baseline fretting fatigue strength of this material. When the test was performed in hydrogen gas, the fretting fatigue strength was significantly reduced as shown by the open symbols. Hydrogen charged into the material caused a further reduction of the fretting fatigue strength as shown by the half-filled symbols. The result showed that environmental hydrogen and hydrogen charged into the material are both important to thoroughly understand the effect of hydrogen on the fretting fatigue strength.

This study focused on the role of environmental hydrogen to reduce fretting fatigue strength of austenitic stainless steel. For this purpose, detailed observations of the adhesion between the contacting surfaces and small cracks were performed. Based on the results of observations, some assumptions concerning the role of hydrogen gas were derived. These assumptions were verified by two-step tests in which the environment was changed during the test.

2. Experimental procedure

2.1. Test material

The test material was an austenitic stainless steel which is designated as SUS304 by Japanese Industrial Standards. The chemical composition is shown in Table 1. In this study, the specimen was made of 30% pre-strained material, since a work-hardened material is frequently used for the mechanical components for high pressure gas to withstand high pressure. The pre-strain was applied to the solution heat-treated material by tensile loading at ambient temperature. The solution heat treatment was done by heating at 1303K for 3.9ks followed by rapid cooling. The mechanical properties of the material are shown in Table 2. The proof strength and tensile strength were significantly increased due to the pre-strain. The Vickers hardness also increased from HV180 to HV338. The microstructures before and after the pre-strain application are shown in Fig. 2. There was a strain-induced martensite microstructure in the pre-strained material. The test specimen was taken from the pre-strained material so that the specimen axis coincided with the tensile load axis. The contact pad was made of the same material.

2.2. Fretting fatigue test

Figure 3 shows the fretting fatigue test method used in the experiment. Two contact pads were pressed onto the front and back side surfaces of the fatigue test specimen. The contact load was adjusted to maintain the constant nominal pressure of 100MPa. The contact load was provided by tightening the bar springs with clamping bolts. The rigidity of the bar springs was carefully designed so that the deflection when the contact

load reached the specified value was sufficiently large compared to the thread lead of the clamping bolt. This enabled close adjustment of the contact load. The fine thread of the clamping bolt also contributed to the precise adjustment of the contact load. While there was a concern that the contact load decreased by development of fretting wear, the contact load was substantially constant during a test, since the depth of the fretting wear was minimal compared to the deflection of the bar springs. After the fretting fatigue test, the actual reduction of the contact load was less than 5% of the initial value.

The fatigue loading type was in-plane bending. The fretting fatigue test was performed with the stress ratio R of -1 at the frequency of 18.7Hz at ambient temperature. The nominal stress amplitude of the specimen was measured by a strain gage pasted on the specimen surface.

The shapes and sizes of the fatigue test specimen and the contact pad are shown in Fig. 4. The contact surfaces of the specimen and the contact pad were finished by buffing to perform close observations of the fretting damage and small fretting fatigue cracks. A square bar type specimen was used in the experiment to obtain a high flatness of the contact surfaces. A bridge type contact pad was used to measure the tangential force. As shown in Fig. 3, a strain gage was pasted at the center of the recessed part of the contact pad. The relationship between the output of the strain gage and tangential force was obtained by a finite-element analysis. The tangential force coefficient was defined as the ratio of the tangential force divided by the contact force.

The test environments were 0.12MPa hydrogen gas and laboratory air. The purity of the hydrogen gas was better than 99.9999%. Prior to the fretting fatigue test in the hydrogen gas, an evacuation sequence of the gas chamber and injection of high purity nitrogen gas were repeated 3 times to maintain the purity of the hydrogen gas. The achieved vacuum was better than 5×10^{-3} Pa.

2.3. Two-step environment test

In the fretting fatigue test in hydrogen gas, failure of the specimen occurred at a lower stress amplitude than the fretting fatigue limit in air. This is one of the most important issues in the design of mechanical components of hydrogen utilization machines. Therefore, the two-step fretting fatigue test in which the environment was changed during the test was performed to examine the cause of the reduction. Table 3 shows the conditions of the two-step test. The stress amplitude of 160MPa was chosen based on the $S-N$ diagram so that the failure of the specimen occurred in the hydrogen gas environment test but did not occur in the air environment test. The No. 1 test attempted to examine the role of the local adhesion to reduce the fretting fatigue strength in the hydrogen gas. Therefore, in the No.1 test, the number of cycles in the first step was chosen for developing an oxidized fretting wear film sufficient enough to prevent adhesion between the contact surfaces. After that, the fretting fatigue test in hydrogen gas was performed. The objective of test No. 2 was to investigate the role of local adhesion to extend the small cracks. Therefore, in test No. 2, the number of cycles in the first step was chosen for introducing 100 μ m deep fretting fatigue cracks. To introduce the pre-cracks with the desired depth, the potential drop technique [5] was used in test No. 2. After the introduction of a pre-crack, the test environment was changed from hydrogen gas to air to release the local adhesion between the contact surfaces. During the second step in both tests, the tests were interrupted at 3×10^7 cycles without failure of the specimen.

3. Examinations of mechanism that causes fretting fatigue damage in hydrogen gas

3.1. *S-N diagram*

The *S-N* diagram of this experiment is shown in Fig. 5. While the number of data points was small, it was sufficient to confirm the reduction of the fretting fatigue strength due to hydrogen gas and to choose the stress amplitude used in the two-step test. The complete *S-N* diagram of this kind of material is given in Ref. [3]. The fretting fatigue limit in air was 180MPa. Since there was a fracture of the specimen in the test performed in the hydrogen gas at the stress amplitude of 160MPa, the fretting fatigue limit in hydrogen gas was speculated to be lower than 160MPa.

In the finite life region where the stress amplitude was higher than the fretting fatigue limit in air, the fretting fatigue life was longer in the hydrogen gas than in air. The reason has been discussed in a previous study [6]. The summary of the discussion is as follows. The nucleation of small fretting fatigue cracks, which were smaller than 10 μ m was within a few percent of the fretting fatigue life for both the hydrogen gas and air environments. However, while the small cracks in the test performed in air steadily propagated after the nucleation, the small cracks in the test done in hydrogen gas were almost arrested. After the arrest of the small cracks, other small cracks nucleated at the inward location of the contact part. This process of nucleation of small cracks and their arrest was repeated until almost 90% of the fretting fatigue life was consumed. Therefore, the reason why the fretting fatigue life in hydrogen gas was longer than that in air was the delay in the start of the stable crack propagation. As for the reason for the arrest of the small cracks in the hydrogen gas, it can be presumed based on the result of the crack propagation test in a vacuum [7] that the crack propagation rate was reduced due to rewelding of the fatigue fracture surfaces.

Change in the fretting wear mechanism depending on the environment was another possible cause of the arrest of the small cracks. It is known that the stress state near the contact edge is significantly affected by the shape of the contact edge. A strong compressive stress field, where small cracks can never propagate, develops in the ideal flat-flat contact [8]. The change in the shape of the contact edge by fretting wear and local plastic deformation releases the concentration of contact pressure at the contact edge which results in the development of a stress field into which the crack can propagate [8, 9]. For the fretting fatigue test in air, it can be considered that the stress field, where small cracks can propagate, promptly developed, since the shape of the contact edge may change during the initial stage of the fretting fatigue life due to fretting wear at the contact edge. As described later, in the fretting fatigue test in hydrogen gas, there was little fretting wear because adhesion was dominant in the process causing the fretting wear damage. Therefore, in the fretting fatigue test in hydrogen gas, the shape of the contact edge may be maintained for a relatively long term. Failure may not occur until the stress field, where small cracks can propagate, develops.

3.2 *Characteristics of fretting damage in hydrogen gas*

Figure 6 shows the morphology of the fretting damage produced in each environment. The observed areas

were in the vicinity of the contact edge. Since the contact surface of the specimen tested in air was covered with oxidized fretting wear particles, the fretted surface was observed after removal of the oxidized fretting wear particles by light buffing. In contrast, there were little fretting wear particles in the hydrogen gas. As shown in the figure, in hydrogen gas, a factory roof-like pattern or chevron pattern whose ridges are perpendicular to the slip direction was observed. This was the specific characteristics of the fretting damage caused in the hydrogen gas.

To elucidate the formation mechanism of the fretting damage in hydrogen gas, matching of the contact surfaces between the specimen and contact pad was performed. Figure 7 shows photographs of the contact surfaces of the specimen and contact pad and surface profiles measured using a confocal microscope. The location of the observations was near the contact edge. The surface profiles were measured on the broken lines in the photographs. The surface asperities exactly matched between the specimen and the contact pad. This suggests that the asperities of the contact surfaces seen in the specimen tested in the hydrogen gas would be produced by transfer of the material. In a vacuum [10] and nitrogen gas [11], it has been reported that the fretting wear mechanism changed from an oxidation dominant process to an adhesion dominant process. Since no oxidized fretting wear particles are produced in hydrogen gas, it is considered that adhesion is dominant, similar to the fretting in a vacuum and nitrogen gas. The area of the damaged parts seemed to be very small compared to the nominal contact area. If the contact load and friction force are transmitted through the adhered spots, it can be presumed that the stress state in the vicinity of the adhered area is very severe.

Figure 8 is a macroscopic indication of the adhesion between the specimen and the contact pad that occurred during the fretting fatigue test in the hydrogen gas. The specimen and the contact pad did not separate even after removal of the contact load.

3.3 Mechanism of reduction of fretting fatigue limit due to hydrogen gas

The adhered specimen and contact pad were rigidly fixed by molding using resin and the mold was then cut in the direction along the specimen axis in order to observe what happened along the contacting interface. Figure 9 shows the longitudinal cross-section of the adhered specimen and contact pad. The cross-section was lightly etched using nitrohydrochloric acid to clearly observe the small cracks.

There were many small cracks at positions A, B and C. The small cracks propagated into both the specimen and the contact pad. In the case of fretting in air, it is known that small oblique cracks and multiple small cracks are the typical characteristics [12]-[14]. When multiple small fretting fatigue cracks are formed in a small area, the angles of propagation of the small cracks are almost constant [15]. However, during fretting fatigue in hydrogen gas, the small cracks propagated in two directions at which the small cracks made angles of approximately 45 or 135 degrees to the contact surface. The morphology of the small cracks in hydrogen gas was distinctly different from that commonly observed during the fretting fatigue test in air.

If the specimen and pad were simply pressed into each other without fretting, a continuous straight line should appear on the cross-section. However, at positions A, B and C, the interface was not continuous and was slightly curved. This was evidence of adhesion. At position A, the interface had a zigzag path due to crosswise overlap of the small cracks which propagated in two directions. Based on this observation, the fretting damage in

hydrogen gas was produced by fatigue cracks. The damage mechanism was not tearing or peeling of the adhered spots when the fretted surfaces were opened. A model of the formation of the fretting damage in hydrogen gas is shown in Fig. 10.

At the position indicated by C in Fig. 9, which was 500 μ m inside from the outer contact edge, there was a major crack leading to specimen failure. The major crack started to propagate from one of the small cracks that emanated from the adhered spot. Therefore, the adhesion and the formation of many small cracks were very important when considering the fretting fatigue strength in the hydrogen gas. For the fretting fatigue in air, the initiation site of small cracks and the direction of crack propagation can be estimated by the mechanical loading conditions including the tangential force, contact force and fatigue load [13] [15]-[18], except when the fretting fatigue cracks emanate from the root of the fretting pits [16]. However, as shown in Fig. 9, small cracks were formed not only at the contact edge, but also over a wide range of the contact surface. In addition, the small cracks propagated in two directions. As a future subject, the quantitative evaluation of the small cracks emanating at the adhered spot is necessary to establish a design method of contact parts in hydrogen utilization machines.

A straight line seen at position D suggests that no adhesion occurred there. Since there are no cracks at this position, the local adhesion has a close relation to the formation of the small cracks.

4. Verification of the role of adhesion and small cracks for the reduction of fretting fatigue limit in hydrogen gas

4.1. Test result for environmental change from air to hydrogen gas

This test was intended to verify the assumption that the prevention of local adhesion between the contact surfaces can produce no reduction in the fretting fatigue limit due to hydrogen gas. The prevention of adhesion was realized by the oxidized film produced by the fretting fatigue cycles in air. After the production of the oxidized fretting wear particles, the environment was changed from air to hydrogen gas. The stress amplitude was intermediate between the fretting fatigue limit in air and that in the hydrogen gas.

The results of the two-step test are shown in Table 4. As a result, there was no failure of the specimen after 10^7 cycles in air and 3×10^7 cycles in the hydrogen gas. The specimen and contact pad were separated without sticking, while they stick together in the hydrogen gas environment test as shown in Fig. 8. The contact surface of this test is shown in Fig. 11. The fretted surface presented a feature similar to that observed in air even though the surface suffered 3×10^7 cycles of fretting in the hydrogen gas. Since the oxidized fretting wear particles prevented the adhesion in the hydrogen gas, the formation of many small cracks was also prevented. Thus, no failure of the specimen occurred even if the stress amplitude was higher than the fretting fatigue limit in the hydrogen gas environment.

4.2. Test result for environmental change from hydrogen gas to air

In the former test, the relation between the adhesion and crack initiation was examined. In the two-step test

No.2, the effect of adhesion on the propagation of small cracks was examined. This test was intended to verify the assumption that the small cracks cannot propagate if the adhesion is eliminated. In this test, small cracks were formed in the hydrogen gas and then the environment was changed to air. The stress amplitude was higher than the fretting fatigue limit in the hydrogen gas environment. That is, the small cracks continued to propagate if the environment was not changed.

As a result, the pre-cracked specimen survived after 3×10^7 cycles of fretting fatigue in air. Figure 12 shows the result of the continuous measurement of the crack length using the electro-potential method in this test. The formation of small cracks and no propagation of the small cracks were confirmed. Based on the results of this test, the elimination of local adhesion prevented a significant increase in the crack length even if the stress amplitude was sufficiently high to cause specimen failure in the hydrogen gas environment. Therefore, it can be considered that the stress state at the contact part was moderated by the elimination of adhesion. Conversely, the stress condition in the vicinity of the small cracks became more severe due to local adhesion.

A quantitative understanding on the small crack observed in the hydrogen gas has not yet been achieved, however, it can be recognized that the stress condition of the contact part is more severe in the hydrogen gas than in air. Figure 13 shows the change in the tangential force coefficient with the change in the environment measured in the two-step test No. 2. The tangential force coefficient is higher in the hydrogen gas than in air.

In Ar gas [19][20] and in a vacuum [21][22], the effect of adhesion on the crack initiation has been reported. Based on this viewpoint, the effect of hydrogen gas on fretting fatigue is similar to those of other non-oxidative environments. However, the fretting fatigue strength did not change in the Ar gas [19][20] and rather increased in the vacuum [23]. In the next step, the difference in the effects between hydrogen gas and other non-oxidative environments will be examined.

5. Conclusions

The mechanism of the reduction in the fretting fatigue limit due to hydrogen gas was investigated by focusing on the change in the damaging process. The material was 30% pre-strained SUS304 austenitic stainless steel. The obtained results are as follows:

- (1) Adhesion is the dominant cause of fretting damage in the hydrogen gas. The major crack leading to specimen failure originated from one of the small cracks that emanated at the adhered spots. The root causes of the reduction in the fretting fatigue strength in the hydrogen gas were local adhesion, the small cracks and increase in the tangential force.
- (2) The prevention of adhesion resulted in no reduction in the fretting fatigue strength in the hydrogen gas. This was caused by the formation of small cracks was prevented.
- (3) The small cracks, which can propagate in the hydrogen gas, became non-propagating cracks in air. It can be considered that the stress conditions in the vicinity of the local adhesion were more severe compared to that in air.

Acknowledgement

This work was supported by the New Energy and Industrial Technology Development Organization (NEDO) in Japan.

References

- [1] Kubota M, Noyama N, Fueta M, Sakae C, Kondo Y, Effect of hydrogen gas environment on fretting fatigue. JSMS 2005; 54 (12): 1231-36.
- [2] Kubota M, Tanaka Y, Kondo Y, Fretting fatigue strength of SCM435H steel and SUH660 heat resistant steel in hydrogen gas environment. Tribotest 2008; 14: 177-91.
- [3] Kubota M, Tanaka Y, Kondo Y, The effect of hydrogen gas environment on fretting fatigue strength of materials used for hydrogen utilization machines. Tribology International 2009; 42: 1352-59.
- [4] Kubota M, Tsuyoshi N, Kondo Y, Effect of hydrogen concentration on fretting fatigue strength. Solid Mechanics and Materials Engineering, Authorized.
- [5] Kondo Y, Kubota M, Sakae C, Yanagihara K, Non-propagating crack at giga-cycle fretting fatigue limit. Fat Fract Engng Mater Struct 2005; 28: 501-6.
- [6] Kubota M, Tanaka Y, Kuwada K, Kondo, Y, Mechanism of reduction of fretting fatigue limit in hydrogen gas environment, Proceedings of the 3rd International Conference on Material and Processing (ICM&P 2008), Northwestern University, Evanston, Illinois, USA 2008.
- [7] Komai K, Matoba H, Kikuchi J, Fatigue crack growth and closure behaviors of high-tensile strength steel in vacuum, Journal of the Society of Materials Science 1984; 33-368: 566-71.
- [8] Nishimura N, Hattori T, Yamashita M, Hasegawa A, Evaluation of fretting wear with finite element method, Proceedings of Japan Society of Mechanical Engineers Annual Meeting, Tokyo 2005; 6: 335-6.
- [9] Kondo Y, Kubota M, Kataoka S, Sakae C, Effect of stress relief groove on fretting fatigue strength and index for the selection of optimal groove shape, International Journal of Fatigue 2009; 31: 439-46.
- [10] Iwabuchi A, Kayaba T, Kato K, Effect of atmospheric pressure of friction and wear of 0.45%C steel in fretting wear. Wear 1983; 91 (3): 289-305.
- [11] Bethune B, Waterhouse RB, Adhesion of metal surfaces under fretting conditions. I. Like metals in contact. Wear 1968; 12: 289-96.
- [12] Nishioka K, Hirakawa K, Fretting fatigue. JSMS 1969; 18 (191): 669-78.
- [13] Endo K, Goto H, Initiation and propagation of fretting fatigue cracks. Wear 1976; 38: 311-24.
- [14] Waterhouse RB, Theories of fretting process, Fretting Fatigue. Edited by Waterhouse RB, Applied Science Publishers, London, UK; 1981, p.203-219.
- [15] Nishioka K, Hirakawa K, Fundamental investigation of fretting fatigue – Part 3. Some phenomena and mechanisms of surface cracks. Bulletin of JSME 1969; 12 (51): 397-407.
- [16] Hirakawa K, Case histories and prevention of fretting fatigue failure. Sumitomo Metals 1994; 46 (4): 4-16.
- [17] Hills DA, Nowell D, Mechanics of fretting fatigue. Kluwer Academic Publishers, Dordrecht, The Netherlands; 1994.
- [18] Xu JQ, Shirai S, Tao WM, Mutoh Y, Initiation and propagation of fretting fatigue crack in the very long

- fatigue life. JSMS 2002; 51 (7): 808-13.
- [19] Endo K, Goto H, Effects of environment on fretting fatigue. Wear 1978; 48: 347-67.
- [20] Wharton MH, Waterhouse RB, Environmental effects in the fretting fatigue of Ti-6Al-4V. Wear 1980; 62: 287-97.
- [21] Poon C, Hoeppner DW, The effect of environment on the mechanism of fretting fatigue. Wear 1979, 52: 175-191.
- [22] Iwabuchi A, Kato K, Kayaba T, Fretting properties of SUS304 stainless steel in a vacuum environment. Wear 1986; 110: 205-16.
- [23] Nishida T, Mutoh Y, Sato M, Kawaguchi K, Fretting fatigue characteristics of aluminum alloy (Al2024-T4) in vacuum. Trans JSME 2009; 75 (756): 981-6.

List of figure captions

Fig. 1. Reduction of fretting fatigue strength of 30% pre-strained SUS304 due to hydrogen [4]:

(a) Fretting fatigue test method and (b) S - N curves.

Fig. 2. Microstructure of material: (a) Solution heat-treated material and (b) 30% re-strained material.

Fig. 3. Fretting fatigue test method used in the experiment.

Fig. 4. Shapes and sizes of the specimen and contact pad (dimensions are in mm):

(a) Fatigue test specimen and (b) bridge type contact pad.

Fig. 5. Effect of hydrogen gas on fretting fatigue limit in hydrogen gas in pre-strained SUS304.

Fig. 6. Morphology of fretting damage ($\sigma_a = 200\text{MPa}$, $N = 10^5$): (a) in air and (b) in H_2 gas.

Fig. 7. Matching of contact surfaces fretted in H_2 . The observed area was in the vicinity of the contact edge:

photographs of (a) photograph and (b) contact pad, and (c) superposition of the surface profiles.

Fig. 8. Adhered specimen and contact pad after fretting fatigue test in H_2 gas ($\sigma_a = 160\text{MPa}$, $N = 1.0 \times 10^7$).

Fig. 9. Observation of adhered part at the section cut in the axial direction ($\sigma_a = 180\text{MPa}$, $N = 1.0 \times 10^6$).

Fig. 10. Model of formation of fretting damage in hydrogen gas: (a) Occurrence of local adhesion and nucleation

of small cracks, (b) Perspective view of (a) to show crack propagation to the direction along the contact

surface and (c) Formation of factory-roof like pattern when the contact surface is opened.

Fig. 11. Fretted surface in the 2-step environment test No. 1

($\sigma_a = 160\text{MPa}$, $N = 10^7$ in air $\rightarrow N = 3 \times 10^7$ in H_2 , not broken).

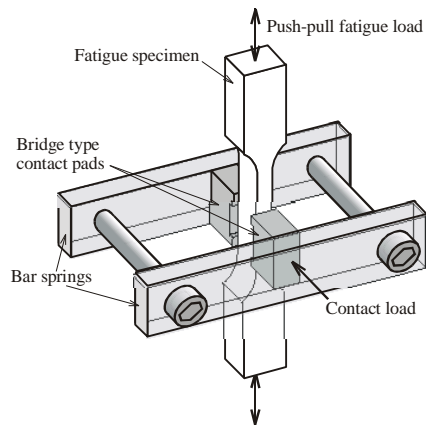
Fig. 12. Confirmation of formation of small cracks and observation of crack propagation

by electro-potential method in the two-step environment test No. 2.

Fig. 13. Comparison of tangential force coefficient between in hydrogen gas and in air

(two step environment test, test No. 2).

a



b

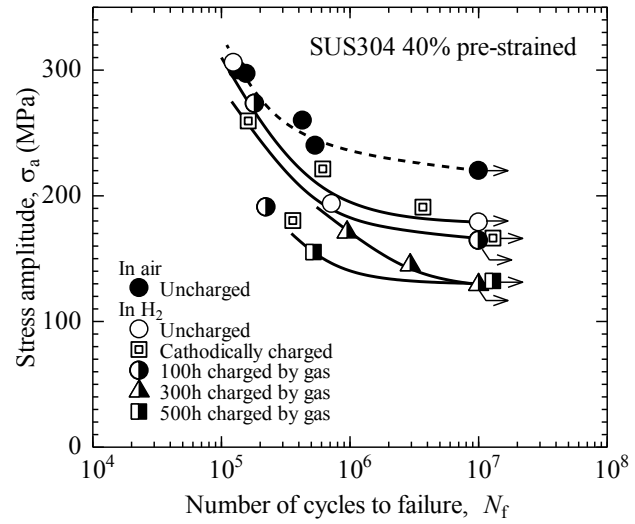


Fig. 1. Reduction of fretting fatigue strength of 30% pre-strained SUS304 due to hydrogen [4]: (a) Fretting fatigue test method and (b) S - N curves

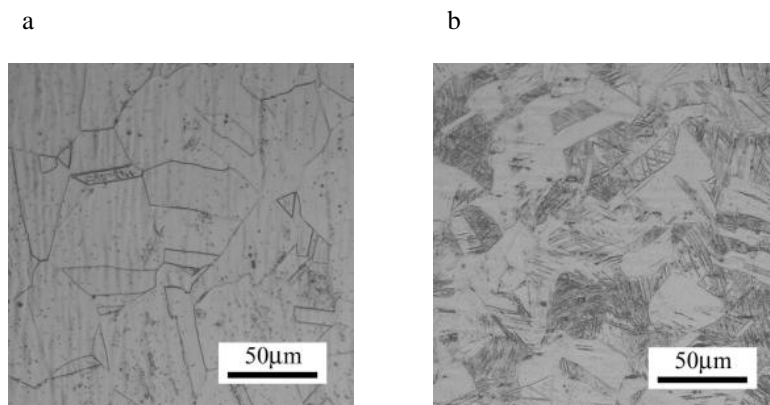


Fig. 2. Microstructure of material: (a) Solution heat-treated material and (b) 30% pre-strained material.

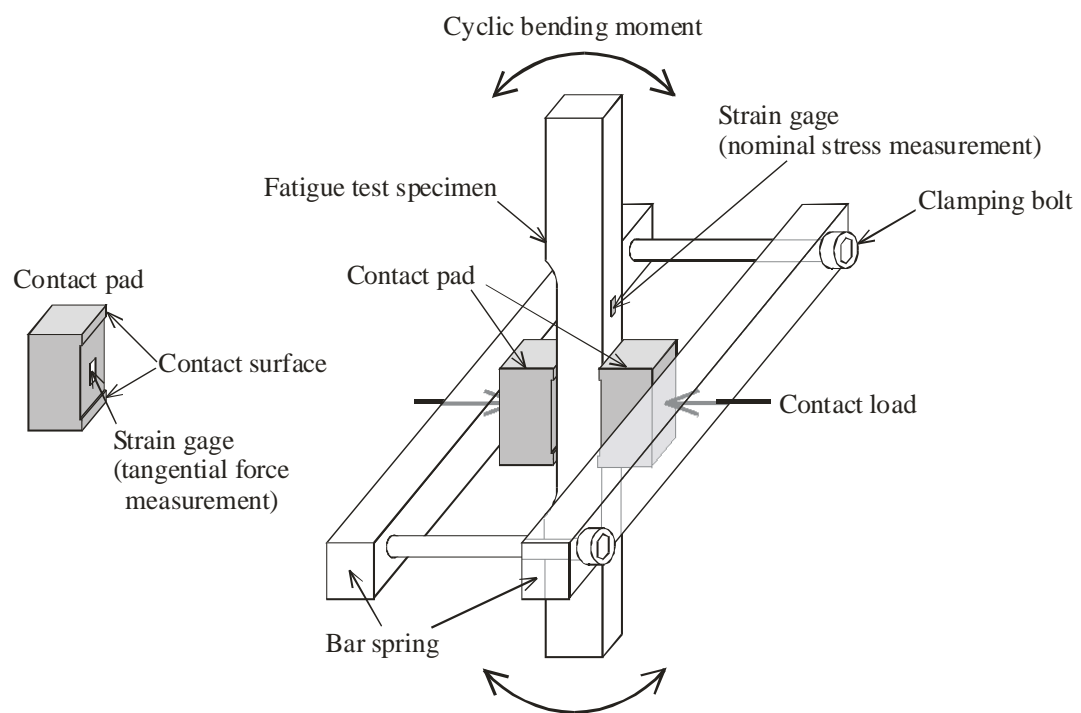
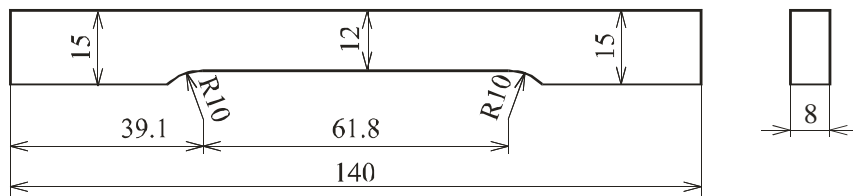


Fig. 3. Fretting fatigue test method used in the experiment.

a



b

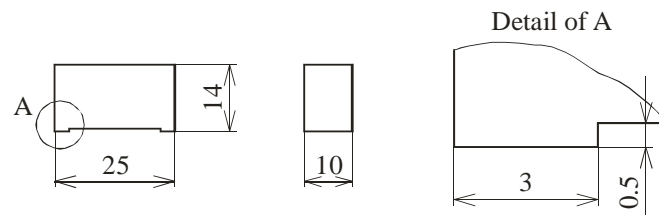


Fig. 4. Shapes and sizes of the specimen and contact pad (dimensions are in mm):

(a) Fatigue test specimen and (b) bridge type contact pad.

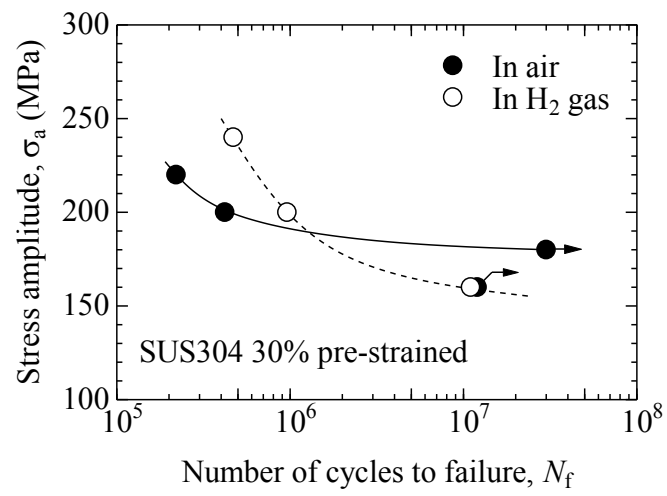
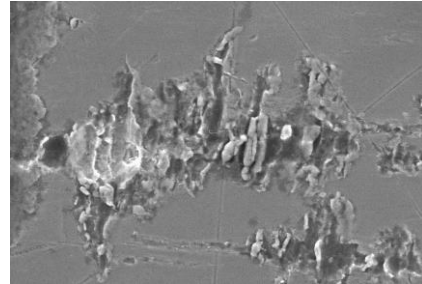
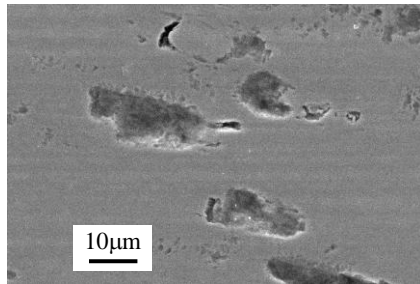


Fig. 5. Effect of hydrogen gas on fretting fatigue limit in hydrogen gas in pre-strained SUS304.

a

b

Outer contact edge→



←→Direction of relative slip

Fig. 6. Morphology of fretting damage ($\sigma_a = 200\text{MPa}$, $N = 10^5$): (a) in air and (b) in H₂ gas.

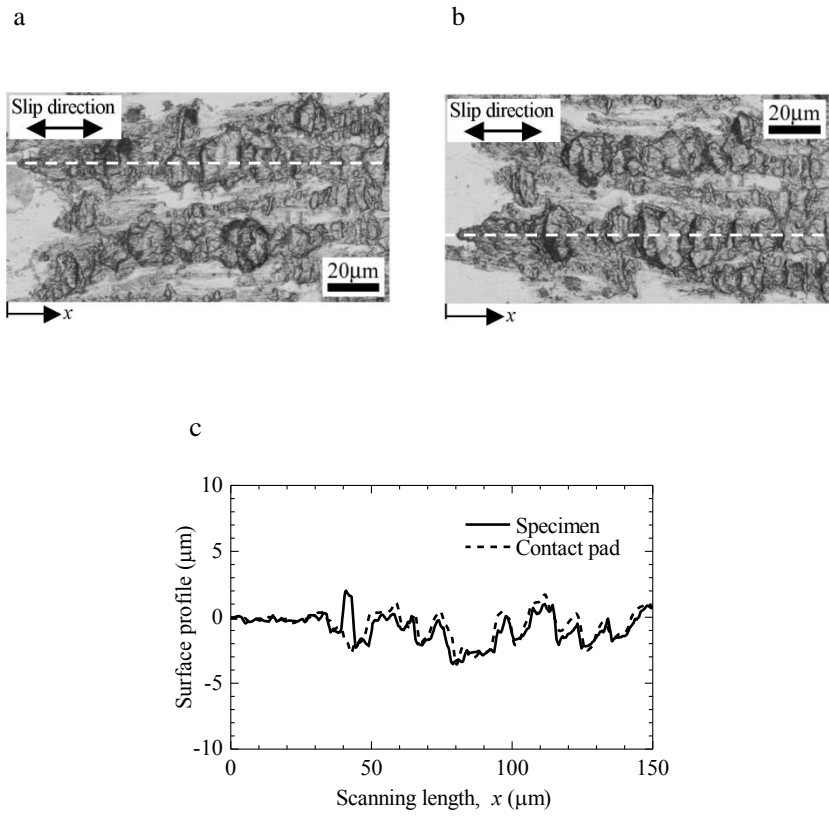


Fig. 7. Matching of contact surfaces fretted in H_2 : photographs of (a) specimen surface and (b) contact pad surface, and (c) superposition of the surface profiles.

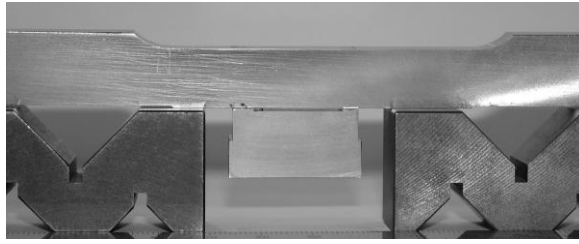


Fig. 8. Adhered specimen and contact pad after fretting fatigue test in H_2 gas ($\sigma_a = 160\text{MPa}$, $N = 1.0 \times 10^7$).

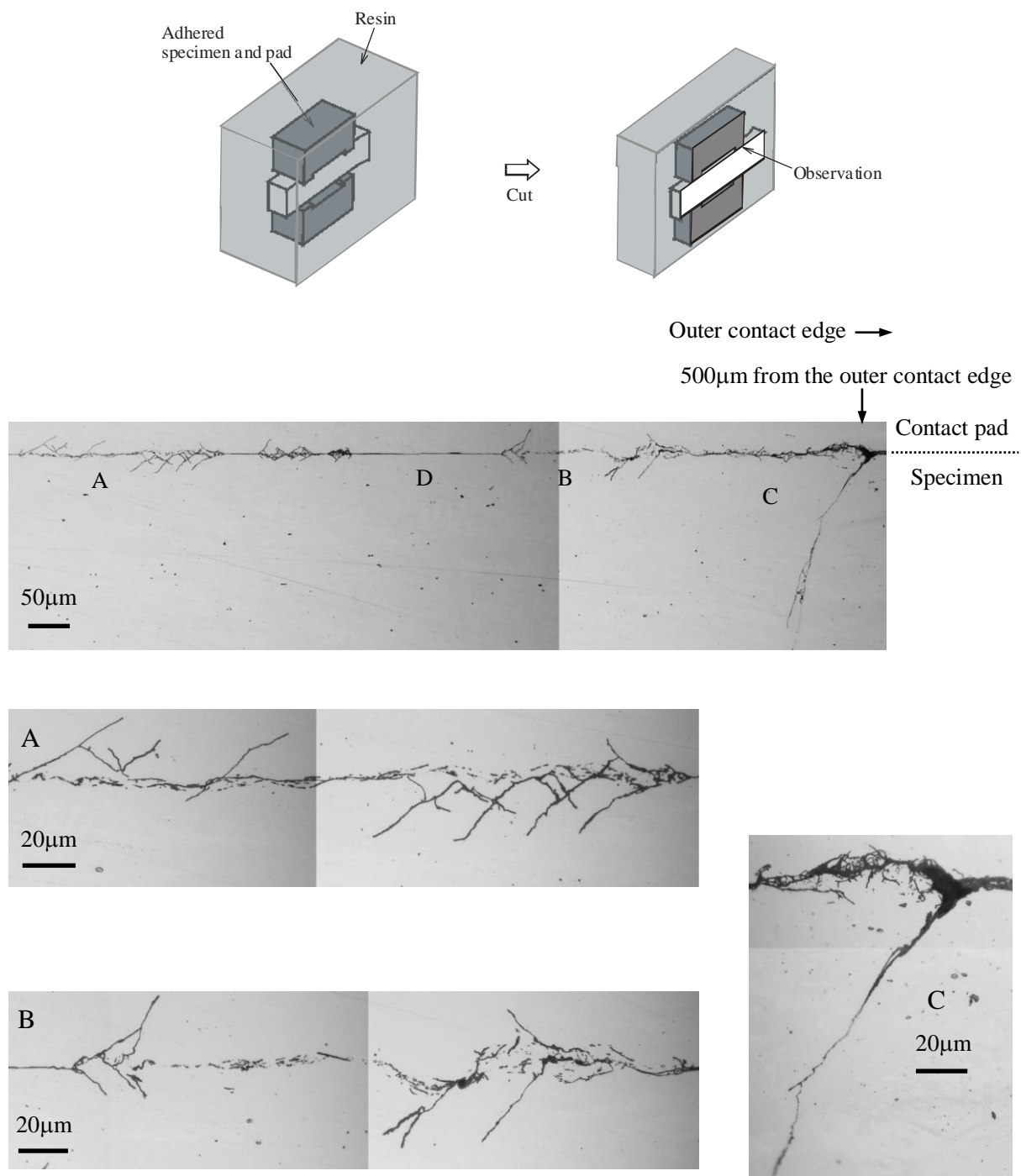


Fig. 9. Observation of adhered part at the section cut in the axial direction ($\sigma_a = 180\text{MPa}$, $N = 1.0 \times 10^6$).

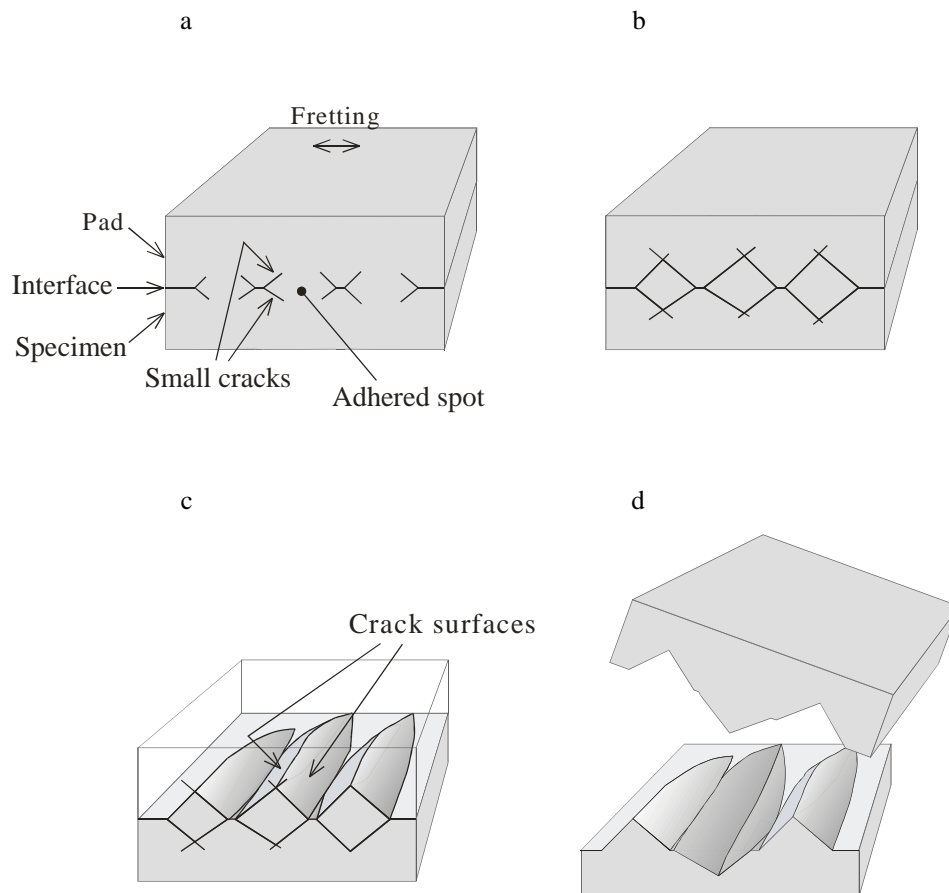


Fig. 10. Model of formation of fretting damage in hydrogen gas:

(a) Occurrence of local adhesion and nucleation of small cracks,

(b) propagation of small cracks,

(c) perspective view of (b) that shows crack propagation to the direction along the contact surface and (d) formation of factory-roof like pattern when the contact surface is opened.

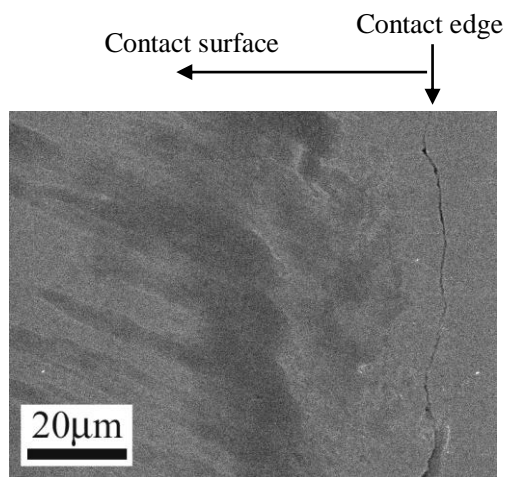


Fig. 11. Fretted surface in the 2-step environment test No. 1
($\sigma_a = 160\text{MPa}$, $N = 10^7$ in air $\rightarrow N = 3 \times 10^7$ in H_2 , not broken).

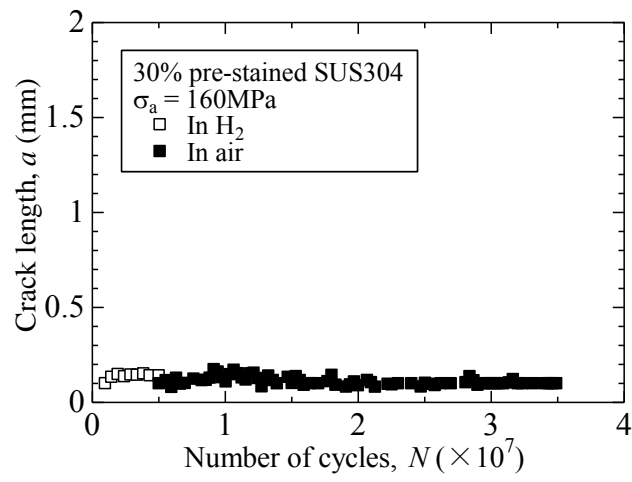


Fig. 12. Confirmation of formation of small cracks and observation of crack propagation by electro-potential method in the two-step environment test No. 2.

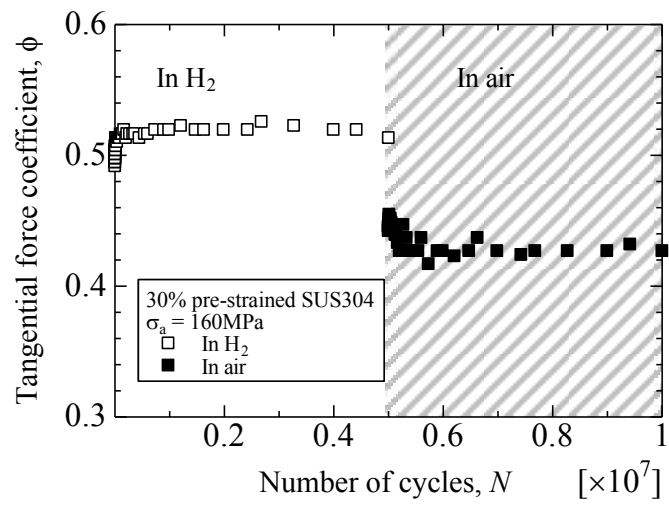


Fig. 13. Comparison of tangential force coefficient between in hydrogen gas and in air (two step environment test test No. 2).

Table 1

Chemical composition of test material (mass%).

| Material | C | Si | Mn | P | S | Ni | Cr |
|----------|------|------|------|-------|-------|------|-------|
| SUS304 | 0.04 | 0.58 | 0.90 | 0.037 | 0.000 | 8.10 | 18.14 |

Table 2

Mechanical properties of test material.

| Material | Condition | 0.2% Proof strength | Tensile strength | Elongation at fracture | Reduction of area |
|----------|------------------|---------------------|------------------|------------------------|-------------------|
| SUS304 | 30% pre-strained | 757MPa | 917MPa | 36% | 74% |

Table 3

Conditions of two-step environment fretting fatigue test.

| Test No. | First step | | | Second step | |
|----------|----------------|------------------------------------|-----------------|----------------|------------------------------------|
| | Environment | Stress amplitude, σ_a (MPa) | N (Cycle) | Environment | Stress amplitude, σ_a (MPa) |
| 1 | Air | 160 | 1×10^7 | H ₂ | 160 |
| 2 | H ₂ | 160 | 5×10^6 | Air | 160 |

* Fretting fatigue limit in air is 180MPa

Table 4

Result of two-step environment fretting fatigue test.

| Test No. | Condition |
|----------|---|
| | Result |
| 1 | In air, $\sigma_a = 160\text{MPa}$, $N = 10^7 \rightarrow$ In H ₂ , $\sigma_a = 160\text{MPa}$ |
| | Not fractured, $N^* = 3 \times 10^7$ |
| 2 | In H ₂ , $\sigma_a = 160\text{MPa}$, $N = 5 \times 10^6 \rightarrow$ In air, $\sigma_a = 160\text{MPa}$ |
| | Not fractured, $N^* = 3 \times 10^7$ |

 N^* is the number of cycles in the 2nd step .